

## N O T I C E

THIS DOCUMENT HAS BEEN REPRODUCED FROM  
MICROFICHE. ALTHOUGH IT IS RECOGNIZED THAT  
CERTAIN PORTIONS ARE ILLEGIBLE, IT IS BEING RELEASED  
IN THE INTEREST OF MAKING AVAILABLE AS MUCH  
INFORMATION AS POSSIBLE

NASA Technical Memorandum 81711

# Effect of Surface Roughness on Hydrodynamic Bearings

(NASA-TM-81711) EFFECT OF SURFACE ROUGHNESS  
ON HYDRODYNAMIC BEARINGS (NASA) 24 P  
HC A02/MF A01 CSCL 13I

N81-21356

Unclas  
G3/37 42073

Bankim C. Majumdar and Bernard J. Hamrock  
*Lewis Research Center  
Cleveland, Ohio*



Prepared for the  
Joint Lubrication Conference  
cosponsored by the American Society of Mechanical Engineers  
and the American Society of Lubrication Engineers  
New Orleans, Louisiana, October 5-7, 1981

**NASA**

# EFFECT OF SURFACE ROUGHNESS ON HYDRODYNAMIC BEARINGS

Bankim C. Majumdar and Bernard J. Hamrock  
National Aeronautics and Space Administration  
Lewis Research Center  
Cleveland, Ohio 44135

## SUMMARY

E-698

A theoretical analysis on the performance of hydrodynamic oil bearings is made considering surface roughness effect. The hydrodynamic as well as asperity contact load is found. Assuming the surface height distribution as Gaussian the contact pressure is calculated. The average Reynolds equation of partially lubricated surface is used to calculate hydrodynamic load. An analytical expression for average gap is found and is introduced to modify the average Reynolds equation. The resulting boundary value problem is then solved numerically by finite difference methods using the method of successive over-relaxation. The pressure distribution and hydrodynamic load capacity of plane slider and journal bearings are calculated for various design data. The effects of attitude and roughness of surface on the bearing performance are shown. The results are compared with similar available solution of rough surface bearings. It is shown that (1) the contribution of contact load is not significant and (2) the hydrodynamic and contact load increase with surface roughness.

## INTRODUCTION

The classical theory of hydrodynamic lubrication given by Reynolds does not consider the surface roughness of the elements having relative motion. This theory is applicable when the bearing surfaces are completely separated by a thick lubricant film. It is known that the bearing load supporting ability increases with decrease in the lubricant film. When the load is very high and the film thickness is small there is a possibility of asperity contact. The method of computation of surface contact load is extremely complex. A few theories concerning the contact of nominally flat surfaces are available [1-4]. In addition to this contact load, the lubricant film between two surfaces having relative motion will also carry a load. This load can be called the hydrodynamic load of a rough surface bearing. There exists two main approaches [5-7] for computation of the hydrodynamic load. Patir and Cheng [5,6] used the flow simulation method of a randomly generated rough surface with known statistical properties over the bearing area. Tønder [7] studied the lubrication of a rough surface by a Monte Carlo method.

The present study uses a flow model similar to Patir and Cheng [5]. This study differs from [6] so far as calculation of average gap  $\bar{h}_T$  is concerned. This gap height is obtained analytically in terms of nominal film thickness,  $h$ . It is then introduced in the basic equation to modify average Reynolds equation. Moreover, the computation of contact load in addition to hydrodynamic load is included. The partial differential equation is solved numerically by finite difference methods satisfying the appropriate bearing boundary conditions. The effect of roughness parameter, attitude, and ratio of correlation length of asperity on the hydrodynamic load capacity is shown.

## NOTATIONS

$A_p$	apparent area of contact [ $m^2$ ]
$B$	width of plane slider [m]
$C$	nominal clearance in journal bearing [m]
$E_a, E_b$	modulus of elasticity of material of surfaces a and b [ $N/m^2$ ]
$\frac{1}{E^*}$	$= \frac{1}{2} \left[ \frac{1 - \nu_a^2}{E_a} + \frac{1 - \nu_b^2}{E_b} \right]$
$e$	eccentricity [m]
$h, H$	nominal film thickness [m], $H = h/h_2$ for slider bearing, $H = h/C$ for journal bearing
$h_1, h_2$	nominal maximum and minimum film thicknesses of slider bearing [m]
$h_T$	local film thickness [m]
$\bar{h}_T$	average film thickness [m]
$K$	a constant
$L$	length of bearing [m]
$N$	number of asperities per unit area
$n$	attitude, $n = h_1/h_2$
$p, P$	mean hydrodynamic pressure [ $N/m^2$ ], $P = (ph_2^2)/(6n\mu B)$ for slider bearing, $P = (pC^2)/(6n\mu K)$ for journal bearing
$p_c$	contact pressure [ $N/m^2$ ]
$R$	journal radius [m]
$t$	time [s]
$u_a, u_b, u$	velocity of surfaces [m/s], $u_a = u$ , $u_b = 0$
$v, V$	squeeze velocity, $v = [-(\partial h)/(\partial t)]$ [m/s], $V = (Bv)/(h_2u)$ for slider bearing, $V = (Rv)/(Cu)$ for journal bearing
$w_c, \bar{w}_c$	asperity contact load [N], $w_c = w_c/LBE'$ for slider bearing, $\bar{w}_c = w_c/2LRE'$ for journal bearing

- $w_h, W_h$  hydrodynamic load [N],  $w_h = (w_h h_2^2)/(6nLB^2u)$  for slider bearing,  
 $w_h$  for journal bearing,  $w_h = (w_h C^2)/(6nLR^2u)$  for journal bearing
- $x, y, X, Y$  coordinates [m],  $X = x/B$ ,  $Y = y/L$
- $R$  mean radius of curvature of asperities [m]
- $\gamma$  ratio of  $x$  and  $y$  correlation length (surface pattern parameter)
- $\Lambda$  roughness parameter,  $\Lambda = h_2/\sigma$  for slider bearing,  $\Lambda = C/\sigma$  for journal bearing
- $\delta_a, \delta_b, \delta$  roughness amplitudes of surfaces measured from their mean levels [m],  $\delta =$  combined roughness,  $\delta = \delta_a + \delta_b$
- $\epsilon$  eccentricity ratio,  $\epsilon = e/C$
- $n$  coefficient of absolute viscosity of lubricant [Ns/m<sup>2</sup>]
- $\nu_a, \nu_b$  Poisson's ratio of material of surfaces  $a$  and  $b$
- $\theta, \theta_2$  angular coordinate (rad),  $\theta = x/R$ ,  $\theta_2 =$  angular coordinate where film breaks
- $\sigma$  standard deviation of combined roughness  $\delta$ ,  $\sigma = \sqrt{\sigma_a^2 + \sigma_b^2}$  or composite rms roughness
- $\sigma_a, \sigma_b$  standard deviations of roughness functions  $\delta_a$  and  $\delta_b$
- $\psi$  attitude angle [rad]
- $\phi_x, \phi_y$  pressure flow factors
- $\phi_s$  shear flow factor

### THEORY

The average Reynolds equation for partial hydrodynamic lubrication is given by Patir and Cheng [5] and it can be written for the surfaces shown in figure 1 as

$$\frac{\partial}{\partial x} \left( \phi_x \frac{h^3}{12n} \frac{\partial p}{\partial x} \right) + \frac{\partial}{\partial y} \left( \phi_y \frac{h^3}{12n} \frac{\partial p}{\partial y} \right) = \frac{u_a + u_b}{2} \frac{\partial \bar{h}_T}{\partial x} + \frac{u_a - u_b}{2} \sigma \frac{\partial \phi_s}{\partial x} + \frac{\partial \bar{h}_T}{\partial t} \quad (1)$$

where

$\sigma$  is the standard deviation  
 $\phi_x$  and  $\phi_y$  are pressure flow factors  
 $\phi_s$  is shear flow factor

The average gap is calculated from

$$\bar{h}_T = \int_{-h}^{\infty} (h + \delta) f(\delta) d\delta \quad (2)$$

where  $f(\delta)$  is probability density function of combined roughness,  $\delta$ . The flow factors  $\phi_x$ ,  $\phi_y$  will approach 1 as  $h/\sigma$  approaches  $\infty$ , whereas  $\phi_s$  will be equal to zero for a large value of  $h/\sigma$ . The average gap  $\bar{h}_T$  is seen to be functions of combined roughness and the probability density function of  $\delta$ . The study to follow will deal with when both surfaces have the same roughness structure and same rms roughness.

To obtain a solution of equation (1) for a particular bearing configuration one has to find  $\phi_x$ ,  $\phi_y$ ,  $\phi_s$ , and  $\bar{h}_T$  beforehand. The  $\phi_x$ ,  $\phi_y$ , and  $\phi_s$  are dependent on the roughness geometry of the bearing surface. The flow factors not only depend on  $h/\sigma$  as mentioned above, they are functions of the statistical properties, such as the frequency density of roughness heights and the directional properties of the asperities. The height distribution is assumed to be Gaussian. The flow factors  $\phi_x$  and  $\phi_y$  are obtained by Patir and Cheng [5] through flow simulation of a rough surface having Gaussian distribution of surface height. These are used in the present case. However, the average gap  $\bar{h}_T$  is calculated in the following way:

For a Gaussian distribution the normal probability density function of  $\delta$  is

$$f(\delta) = \frac{1}{\sigma\sqrt{2\pi}} e^{-\frac{\delta^2}{2\sigma^2}} \quad (3)$$

where  $\sigma$  is the standard deviation.

Substituting equation (3) into equation (2),

$$\bar{h}_T = \frac{1}{\sigma\sqrt{2\pi}} \int_{-h}^{\infty} (h + \delta) e^{-\frac{\delta^2}{2\sigma^2}} d\delta$$

After performing the above integration, we get  $\bar{h}_T$  as

$$\bar{h}_T = \frac{h}{2} \left[ 1 + \operatorname{erf} \left( \frac{h}{\sqrt{2}\sigma} \right) \right] + \frac{\sigma}{\sqrt{2\pi}} e^{-\frac{h^2}{2\sigma^2}} \quad (4)$$

since

$$\frac{1}{\sqrt{\pi}} \int_h^{\infty} e^{-r^2} dr = \frac{1}{2} [1 - \text{erf}(h)]$$

Differentiating  $\bar{h}_T$  with respect to  $x$ , one obtains

$$\frac{\partial \bar{h}_T}{\partial x} = \frac{1}{2} \left[ 1 + \text{erf} \left( \frac{h}{\sqrt{2}\sigma} \right) \right] \frac{\partial h}{\partial x} \quad (5)$$

Similarly

$$\frac{\partial \bar{h}_T}{\partial t} = \frac{1}{2} \left[ 1 + \text{erf} \left( \frac{h}{\sqrt{2}\sigma} \right) \right] \frac{\partial h}{\partial t} \quad (6)$$

The flow simulation factors  $\phi_x$ ,  $\phi_y$ , and  $\phi_s$  are given by [5,6],

$$\phi_x = 1 - C_1 e^{-r \left( \frac{h}{\sigma} \right)} \quad \text{for } \gamma \leq 1$$

$$\phi_x = 1 + C_1 \left( \frac{h}{\sigma} \right)^{-r} \quad \text{for } \gamma > 1$$

$$\phi_s = A_1 \left( \frac{h}{\sigma} \right)^{\alpha_1} e^{-\alpha_2 \left( \frac{h}{\sigma} \right) + \alpha_3 \left( \frac{h}{\sigma} \right)^2} \quad \text{for } \frac{h}{\sigma} \leq 5 \quad (7)$$

$$\phi_s = A_2 e^{-\alpha_4 \left( \frac{h}{\sigma} \right)} \quad \text{for } \frac{h}{\sigma} > 5$$

and

$$\phi_y \left( \frac{h}{\sigma}, \gamma \right) = \phi_x \left( \frac{h}{\sigma}, \frac{1}{\gamma} \right)$$

where  $C_1$ ,  $r$ ,  $A_1$ ,  $A_2$ ,  $\alpha_1$ ,  $\alpha_2$ ,  $\alpha_3$ , and  $\alpha_4$  are constants and tabulated in [6], and  $\gamma$  is defined as ratio of lengths at which the auto-correlation function of the  $x$  and  $y$  profiles reduce to 50 percent of the initial value. This  $\gamma$  can be thought of as the length-to-width ratio of a representative asperity. For isotropic roughness  $\gamma = 1$ .

Having known the flow factors and  $\bar{h}_T$ ; and assuming  $u_b = 0$  and  $u_a = u$  equation (1) for constant  $n$  and when both surfaces have same roughness structure can be written as

$$\frac{\partial}{\partial x} \left( \phi_x h^3 \frac{\partial p}{\partial x} \right) + \frac{\partial}{\partial x} \left( \phi_y h^3 \frac{\partial p}{\partial y} \right) = 6n \left\{ \frac{1}{2} \left[ 1 + \operatorname{erf} \left( \frac{h}{\sqrt{2}\sigma} \right) \right] \left( u \frac{\partial h}{\partial x} + \frac{\partial h}{\partial t} \right) \right\} \quad (8)$$

It has been found in [6] that for the type of model as mentioned earlier (i.e., when both surfaces have same roughness structure) there is no  $\phi_s$  effect.

Let us now attempt to find the solution of equation (8) for the infinitely long plane slider, finite plane slider, and infinitely long journal bearing.

### Infinitely Long Plane Slider Bearing

Figure 2 shows a slider bearing. If length of the slider is very long compared to  $B$ ,  $\partial p / \partial y = 0$ . Hence equation (8) can be written as

$$\frac{\partial}{\partial x} \left( \phi_x h^3 \frac{\partial p}{\partial x} \right) = 6n \left\{ \frac{1}{2} \left[ 1 + \operatorname{erf} \left( \frac{h}{\sqrt{2}\sigma} \right) \right] \left( u \frac{\partial h}{\partial x} + \frac{\partial h}{\partial t} \right) \right\} \quad (9)$$

Using the following substitutions:

$$X = \frac{x}{B}, \quad \Lambda = \frac{h_2}{\sigma}, \quad H = \frac{h}{h_2}, \quad \text{and} \quad P = \frac{\rho h_2^2}{6\eta u B}$$

equation (9) becomes

$$\frac{\partial}{\partial X} \left( \phi_x H^3 \frac{\partial P}{\partial X} \right) = \frac{1}{2} \left[ 1 + \operatorname{erf} \left( \frac{\Lambda H}{\sqrt{2}} \right) \right] \left( \frac{\partial H}{\partial X} - \frac{Bv}{h_2 u} \right) \quad (10)$$

since  $v = -(\partial h / \partial t)$ .

Expanding equation (10),

$$\phi_x H^3 \frac{\partial^2 P}{\partial X^2} + 3\phi_x H^2 \frac{\partial P}{\partial X} \frac{\partial H}{\partial X} + H^3 \frac{\partial P}{\partial X} \frac{\partial \phi_x}{\partial X} = \frac{1}{2} \left[ 1 + \operatorname{erf} \left( \frac{\Lambda H}{\sqrt{2}} \right) \right] \left( \frac{\partial H}{\partial X} - v \right) \quad (11)$$

where

$$v = \frac{Bv}{h_2 u}$$

The dimensionless parameter  $v$  can be visualized as squeeze effect and it comes from the flow continuity.

For a slider bearing, the dimensionless film thickness,  $H$  is given by

$$H = n - (n - 1)X \quad (12)$$

where  $n = h_1/h_2$ .

The bearing boundary conditions are



$$P = 0 \quad \text{at} \quad X = 0 \quad (13)$$

and

$$P = 0 \quad \text{at} \quad X = 1$$

### Finite Slider Bearing

The dimensionless differential equation in this case will be

$$\begin{aligned} \phi_x H^3 \frac{\partial^2 P}{\partial X^2} + 3\phi_x H^2 \frac{\partial P}{\partial X} \frac{\partial H}{\partial X} + H^3 \frac{\partial P}{\partial X} \frac{\partial \phi_x}{\partial X} + \left(\frac{B}{L}\right)^2 \phi_y H^3 \frac{\partial^2 P}{\partial Y^2} \\ = \frac{1}{2} \left[ 1 + \operatorname{erf} \left( \frac{\Lambda H}{\sqrt{2}} \right) \right] \left( \frac{\partial H}{\partial X} - V \right) \end{aligned} \quad (14)$$

where  $Y = y/L$ .

The film thickness  $H$ , and the bearing boundary conditions are still given by equations (12) and (13) with additional boundary conditions at the sides.

### Infinitely Long Journal Bearing

A journal bearing as shown in figure 3 when rotating with velocity  $u$  carries a load  $w$ . If the length of the bearing is large compared to other dimensions, then there will be no side leakage. Thus when  $L/R$  is large,  $\partial P / \partial y = 0$ . Therefore the basic equation will be equation (9). This can be nondimensionalized with the following substitutions:

$$\theta = \frac{x}{R}, \quad H = \frac{h}{C}, \quad \Lambda = \frac{C}{\sigma}, \quad \text{and} \quad P = \frac{\rho C^2}{6\eta u R}$$

The dimensionless equation is

$$\phi_x H^3 \frac{\partial^2 P}{\partial \theta^2} + 3\phi_x H^2 \frac{\partial H}{\partial \theta} \frac{\partial P}{\partial \theta} + H^3 \frac{\partial P}{\partial \theta} \frac{\partial \phi_x}{\partial \theta} = \frac{1}{2} \left[ 1 + \operatorname{erf} \left( \frac{\Lambda H}{\sqrt{2}} \right) \right] \left( \frac{\partial H}{\partial \theta} - V \right) \quad (15)$$

where

$$H = 1 + \epsilon \cos \theta, \quad \epsilon = \frac{e}{C}, \quad V = \frac{Rv}{Cu} \quad (16)$$

The boundary conditions are:

$$\begin{aligned} P = 0 \quad \text{at} \quad \theta = 0 \\ P = \frac{\partial P}{\partial \theta} = 0 \quad \text{at} \quad \theta = \theta_2 \end{aligned} \quad (17)$$

where  $\theta_2$  is the angular coordinate at which the film breaks. This boundary condition is known as Reynolds condition. Using the expression of  $H$ , equation (15) can be reduced to

$$\begin{aligned} \phi_x (1 + \epsilon \cos \theta)^3 \frac{\partial^2 p}{\partial \theta^2} - 3\epsilon \phi_x (1 + \epsilon \cos \theta)^2 \sin \theta \frac{\partial p}{\partial \theta} + (1 + \epsilon \cos \theta)^3 \frac{\partial p}{\partial \theta} \frac{\partial \phi_x}{\partial \theta} \\ = \frac{1}{2} \left[ 1 + \operatorname{erf} \left( \frac{\Lambda H}{\sqrt{2}} \right) \right] (-\epsilon \sin \theta - V) \end{aligned} \quad (18)$$

Equations (11), (14), and (18) are solved numerically by finite difference methods with successive over-relaxation factor satisfying the appropriate boundary conditions for infinitely long plane slider, finite plane slider, and infinitely long journal bearing, respectively.

#### Calculation of Hydrodynamic Load

With the known hydrodynamic pressure distribution the hydrodynamic load can be calculated from:

For infinitely long plane slider -

$$\begin{aligned} w_h &= L \int_0^B p \, dx \\ &= \frac{6nLB^2u}{h_2^2} \int_0^1 P \, dX \end{aligned}$$

or

$$w_h = \int_0^1 P \, dX \quad (19)$$

where

$$w_h = \frac{w_h n_2^2}{6nLB^2u}$$

For finite plane slider -

$$w_h = \int_0^1 \int_0^1 P \, dX \, dY \quad (20)$$

where  $w_h$  is defined the same as for the infinite slider.

For infinitely long journal bearing the two components of loads are -

$$w_{hr} = -LR \int_0^{\theta_2} p \cos \theta \, d\theta$$

and

$$w_{he} = LR \int_0^{\theta_2} p \sin \theta \, d\theta$$

These can be written in dimensionless form as

$$W_{hr} = - \int_0^{\theta_2} P \cos \theta \, d\theta$$

and

$$W_{he} = \int_0^{\theta_2} P \sin \theta \, d\theta$$

(21)

The total hydrodynamic load is

$$W_h = \sqrt{W_{hr}^2 + W_{he}^2} \quad (22)$$

where

$$W_h = \frac{w_h C^2}{6nLR^2u}$$

The attitude angle

$$\psi = \tan^{-1} \left( \frac{W_{he}}{W_{hr}} \right) \quad (23)$$

The integrations of equations (19), (20), and (21) are performed numerically by Simpson's rule.

#### Calculation of Asperity Contact Load

Using a Gaussian distribution of asperity height, the contact load can be evaluated from the nominal contact pressure. When both surfaces are rough, the nominal pressure can be obtained from Greenwood and Tripp [4]. This is written as

$$p_c = KE'F_{5/2}(\Lambda) \quad (24)$$

where

$$K = \frac{8\sqrt{2}}{15} \pi (N\beta\sigma)^2 \sqrt{\frac{\sigma}{\beta}}$$

N number of asperities per unit area

$\beta$  mean radius of curvature of asperities

E' composite modulus of elasticity

and

$$F_{5/2} = \frac{1}{\sqrt{2\pi}} \int_{\Lambda}^{\infty} (s - \Lambda)^{5/2} e^{-(s - \Lambda)^2/2} ds$$

The value of K varies from 0.003 to 0.0003 for the range of  $\sigma/\beta$  between 0.01 and 0.001. The function  $F_{5/2}$  has been calculated in [4] and is reproduced below for various  $\Lambda$ .

$\Lambda$	$F_{5/2}$
0	0.61664
.5	.24040
1.0	.08056
1.5	.02286
2.0	.00542
2.5	.00106
3.0	.00017
3.5	.00002
4.0	.00000

The contact load is

$$w_c = A_p p_c \quad (25)$$

where  $A_p$  is the apparent area of contact.  
Therefore for plane slider bearing

$$w_c = LB p_c \quad (26)$$

or

$$w_c = KF_{5/2}$$

where

$$w_c = \frac{w_c}{LBE}$$

Similarly for journal bearing  $W_c$  is given by

$$W_c = \frac{W_c}{2LRE^T}$$

where  $W_c = 2LRp_c$ .

The above two dimensionless loads  $W_h$  and  $W_c$  are defined with different physical parameters. Therefore these cannot be simply added in this form. In the following section an example is taken to show the effect of  $W_c$  and  $W_h$ . The discussion to follow is concerning  $W_h$ .

## RESULTS AND DISCUSSION

The hydrodynamic load has been calculated using the foregoing method for infinitely long plane slider, finite slider, and infinitely long journal bearings. The example given later shows that the asperity contact load is much smaller than the hydrodynamic load. Therefore the results are given with respect to  $W_h$  only.

Figures 4 to 10 show the results of plane slider bearings and the results for the journal bearing are given in table I and figure 11. It may be noted the results corresponding to  $\Lambda = 6$  approach the smooth bearing solutions.

### Plane Slider Bearing

The effect of various parameters, namely,  $n$ ,  $V$ ,  $L/B$ ,  $\Lambda$  and  $\gamma$  on  $W_h$  is discussed in the following paragraphs.

(1) Effect of roughness parameter  $\Lambda$ : Each of the figures shows that the hydrodynamic load is increased with decrease in the  $\Lambda$ . This increase is due to pressure flow effect ( $\phi_x$  and  $\phi_y$ ) and the extra term in the average gap  $\bar{h}_T$ . The hydrodynamic load also increases very sharply at small  $\Lambda$ .

(2) Effect of attitude  $n$ : When local squeeze term  $V$  is neglected, the load capacity is maximum at  $n = 2$  for most values of  $\Lambda$ . The variation of load with  $n$  for a particular  $\Lambda$  is more or less similar to that of a smooth bearing. It may be mentioned that an infinitely long plane slider having smooth surfaces carries a maximum load when  $n = 2.2$ . In the present case the load reaches a maximum value when  $n$  varies between 2.0 and 2.5.

(3) Effect of local squeeze velocity  $V$ : The effect of squeeze velocity is always to enhance the load. In rough surface bearings (figs. 4 and 5) the similar effect is also seen. From figure 5 it may be noticed that a bearing operating on small attitude gives high load. This indicates that for a bearing having nearly parallel film, the squeeze velocity plays a significant role so far as load capacity is concerned.

(4) Effect of length to width ratio  $L/B$ : The hydrodynamic load increases with the  $L/B$  ratio (fig. 9). This is expected from the physical point of view. However, load does not consistently change with the change of  $L/B$  ratio.

(5) Effect of surface pattern parameter  $\gamma$ : The  $\gamma$  parameter represents the directional properties of surfaces. As  $\gamma$  is the ratio of length-to-width of an asperity and as the orientation of asperity disturbs the flow, its effect on the load is seen to predominant (fig. 10). As per definition purely transverse, isotropic and longitudinal roughness patterns

correspond to  $\gamma = 0, 1$  and  $\infty$ , respectively. As the values of pressure flow factor  $\phi_x$  are known from 1/6 to 6, these are used here. These two values adequately represent transverse and longitudinal patterns. For a square bearing the maximum and minimum load are obtained with isotropic and longitudinal surface roughness, respectively. Whereas the surfaces with transverse pattern give intermediate values.

#### Approximate Equation

From a near optimum slider ( $n = 2$ ) it has been found that the load capacity of isotropic rough and smooth surfaces can be closely approximated by the following simple relationship:

$$W_{h(\text{rough})} = \frac{W_{h(\text{smooth})}}{1 - 0.77 e^{-0.76 \Lambda}} \quad (27)$$

The maximum error introduced by this approximation is about 5 percent.

#### Journal Bearing

The hydrodynamic load, attitude angle, and the location of lubricating film breakdown for an infinitely long journal bearing using Reynolds boundary conditions are given in table I and figure 11. The load capacity increases with decrease in the  $C/\sigma$  (or  $\Lambda$ ) ratio, but the extents of lubricating film in most cases do not change. The attitude angle drops very slowly with increase in the roughness. Due to this reason the variation of  $\phi$  and  $\theta_2$  is given in table I. The variation of load, attitude angle, and the extent of film with eccentricity ratio is very much similar to that of a smooth bearing.

#### Calculation of Total Load ( $w_h + w_c$ )

The dimensionless hydrodynamic and contact loads are defined in such a way one cannot add them directly. The relative load sharing ability is shown with an illustrative example.

Example:

A plane slider bearing made of steel is operating under the following conditions:

Length of bearing  $L = 50$  mm

width of bearing  $B = 50$  mm

Minimum film thickness  $h_2 = 5 \times 10^{-6}$  m

Attitude  $n = 2.0$

Sliding speed  $u = 5$  m/s

Absolute viscosity of oil  $\eta = 0.20$  Ns/m<sup>2</sup>

The hydrodynamic and contact load for the above bearings are calculated.

Assume  $E' = 2.2 \times 10^{11}$  N/m<sup>2</sup>.

The hydrodynamic load is given by the expression:

$$w_h = \frac{6nLB^2u}{h_2^2} w_h [N]$$

Substituting the above data in this expression

$$w_h = 30 \times 10^6 w_h [N]$$

The contact load can be written as

$$w_c = LBKE'F_{5/2} [N]$$

Although  $F_{5/2}$  will be slightly different from  $h_2$  to  $h_1$ ,  $F_{5/2}$  at  $h_2$  is used here. Taking  $K = 0.003$ , assuming isotropic surface roughness and using the above data

$$w_c = 165 \times 10^4 F_{5/2} [N]$$

For various roughness parameters the hydrodynamic and contact load are calculated for isotropic surface roughness and are shown below:

$\Lambda (=h_2/\sigma)$	$w_h [kN]$	$w_c [kN]$	$w_c/w_h$
1	453	133	0.294
2	360	8.94	.0248
3	321	.28	.00086
6	300	0	0

#### Comparison of Results

The hydrodynamic load capacity for the square plane slider with  $n = 2$  and  $\gamma = 1$  is compared with that of Patir and Cheng [6] result. These are shown in table II. The Patir and Cheng results are slightly higher than those obtained from the present method of solution. All the data in table II are in agreement within 20 percent. The load capacity corresponding to other values of  $\Lambda$  are consistently higher. This may be due to assumption of polynomial density function for the Gaussian function in the calculation of  $\bar{h}_T$  in [6]. The present calculations are, however, made from the exact expression of  $\bar{h}_T$  (eq. (4)). Again the numerical calculation are done with an accuracy of 0.01 percent of the difference of integrated pressures of two successive iterations. Therefore, it is believed that the present data give good accuracy.

#### CONCLUSIONS

Loads due to asperity contact as well as hydrodynamic pressure were considered in studying the effect of surface roughness on hydrodynamic bearings. The height distribution was assumed to be Gaussian and the contact pressure was calculated. The average Reynolds equation with flow simulation

of a randomly generated rough surface was used to calculate the hydrodynamic load. An analytical expression for the average gap was found and was introduced in the modified average Reynolds equation. The pressure distribution and hydrodynamic load capacity of plane slider and journal bearings are estimated for various design data. The effect of attitude and ratio of film thickness to standard deviation of a surface was shown. The following conclusions are drawn from the above analysis.

1. Both the hydrodynamic and contact load increase with increase in the surface roughness.

2. For a square plane slider maximum hydrodynamic load is observed with isotropic surface roughness.

3. The hydrodynamic load approaches to a smooth bearing solution when  $\Lambda = 6$  and the contact load approaches zero when  $\Lambda = 4$ .

4. Although the hydrodynamic load of journal bearing varies with surface roughness, there is little variation of attitude angle and the location of the point of film breakdown.

5. The approximate equation proposed for plane slider bearing having  $n = 2$  may be used for design calculations.

#### ACKNOWLEDGEMENT

During the period when the work described in this paper was carried out, one of the authors (B. C. Majumdar) was in receipt of a National Research Council Senior Research Associateship and located in the Mechanical Technologies Branch of NASA Lewis Research Center in Cleveland, Ohio.

#### REFERENCES

1. Greenwood, J. A. and Williamson, J. B. P., "Contact of Nominally Flat Rough Surfaces," Proceedings of the Royal Society, London, Vol. A295, No. 1442, Dec. 1966, pp. 300-319.
2. Whitehouse, D. J. and Archard, J. F., "The Properties of Random Surfaces of Significance in Their Contact," Proceedings of the Royal Society, London, Vol. A316, No. 1524, Mar. 1970, pp. 97-121.
3. Nayak, P. R., "Random Process Model of Rough Surfaces," Journal of Lubrication Technology, ASME Trans., Vol. 93, No. 3, July 1971, pp. 398-407.
4. Greenwood J. A. and Tripp, J. H., "The Contact of Two Nominally Flat Rough Surfaces," Proceedings of the Institution of Mechanical Engineers, London, Vol. 185, 1970-71, pp. 625-633.
5. Patir, N. and Cheng, H. S., "An Average Flow Model for Determining Effects of Three-Dimensional Roughness on Partial Hydrodynamic Lubrication," Journal of Lubrication Technology, ASME Trans., Vol. 100, No. 1, Jan. 1978, pp. 12-17.
6. Patir, N. and Cheng, H. S., "Application of Average Flow Model to Lubrication Between Rough Sliding Surfaces," Journal of Lubrication Technology, ASME Trans., Vol. 101, No. 2, Apr. 1979, pp. 220-230.
7. Tønder, K., "Simulation of the Lubrication of Isotropically Rough Surfaces," American Society for Lubrication Engineers, Trans., Vol. 23, No. 3, July 1980, pp. 326-333.



TABLE I. - PERFORMANCE CHARACTERISTICS OF INFINITELY LONG  
JOURNAL BEARING ( $V = 0$ )

$\epsilon$	$\Lambda$	$W_h$	$\theta_2^{\circ}$	$\psi^{\circ}$
0.1	1	0.361	247	71.770
	2	.269	247	71.800
	3	.252	247	71.861
	4	.233	247	71.934
	6	.218	247	72.030
0.2	1	0.699	237	68.999
	2	.564	237	69.070
	3	.494	237	69.206
	4	.457	240	69.370
	6	.427	240	69.580
0.4	1	1.346	220	62.323
	2	1.104	222	62.526
	3	.981	222	62.817
	4	.913	225	63.185
	6	.855	225	63.700
0.6	1	2.184	210	53.089
	2	1.803	210	53.562
	3	1.632	210	54.018
	4	1.530	210	54.542
	6	1.423	210	55.379
0.8	1	4.538	197	38.676
	2	3.656	197	39.481
	3	3.301	197	40.145
	4	3.099	197	40.671
	6	2.863	197	41.482

TABLE II. - COMPARISON OF HYDRODYNAMIC LOAD CAPACITY OF  
FINITE SLIDER BEARING ( $L/B = 1$ ,  $n = 2$ ,  $\gamma = 1$ )

$\Lambda$	$W_h$	
	Patir and Cheng [6]	Present
1	0.0182	0.0151
2	.0146	.0120
3	.0130	.0107
6	.0115	.010

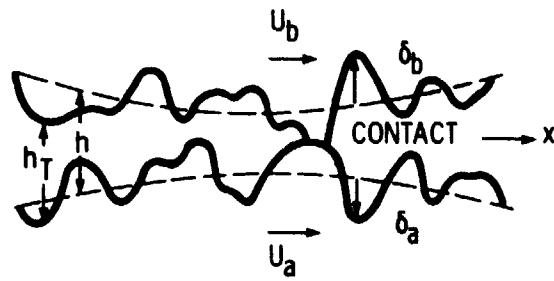


Figure 1. Film geometry.

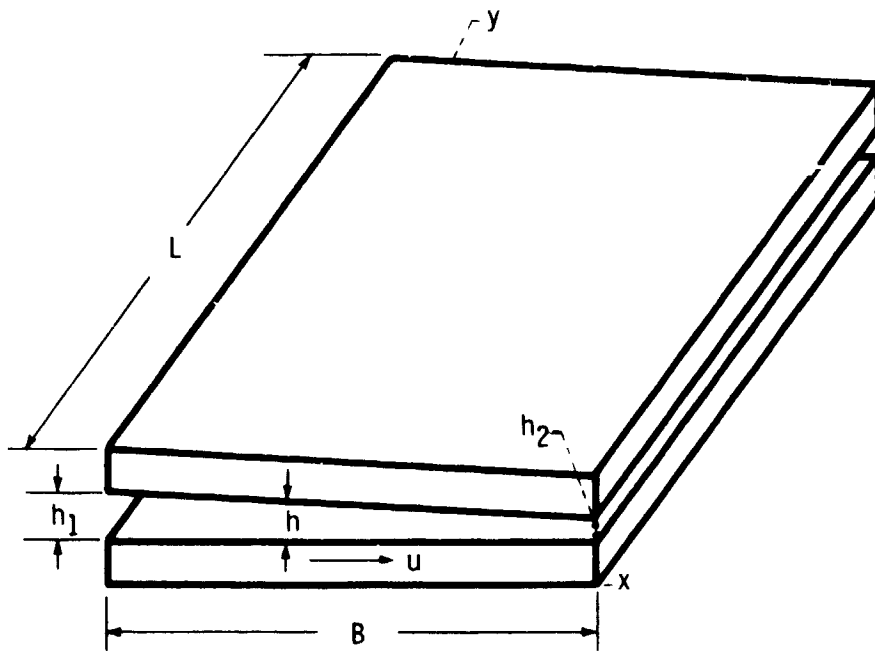


Figure 2. - A plane slider bearing.

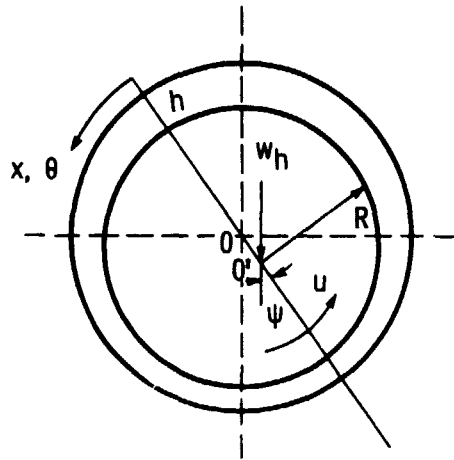


Figure 3. - A journal bearing.

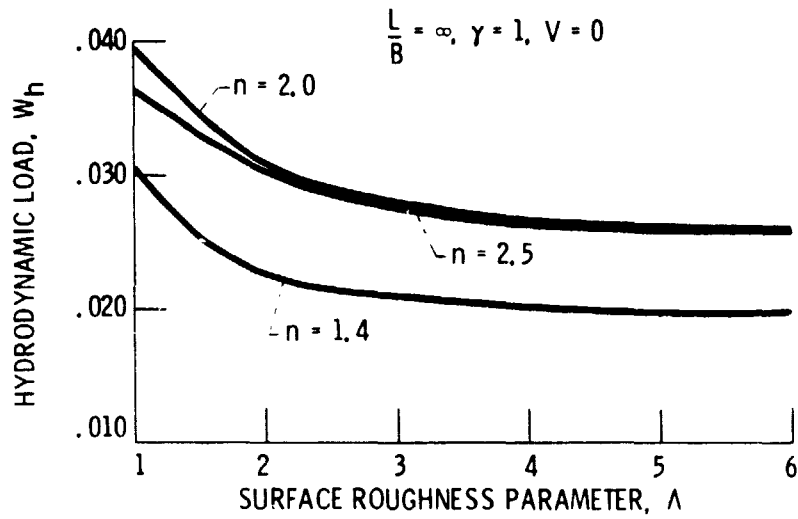


Figure 4. - Variation of hydrodynamic load with surface roughness parameter for various attitudes.

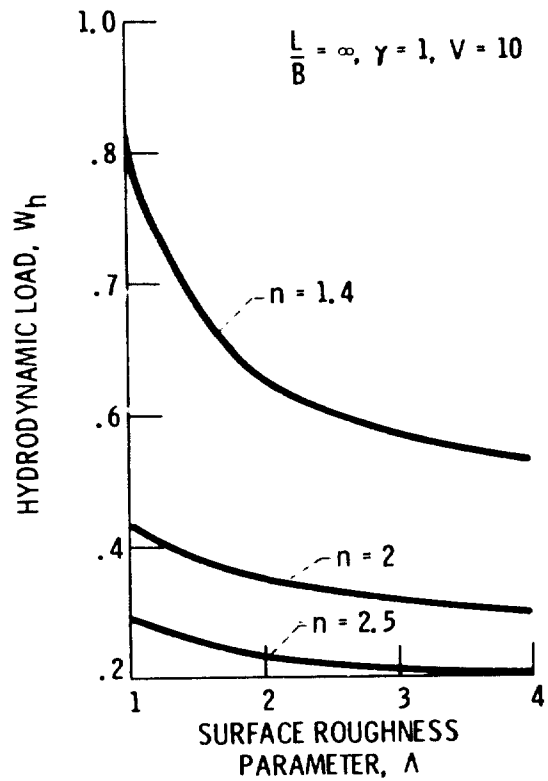


Figure 5. - Variation of hydrodynamic load with surface roughness parameter for various attitudes.

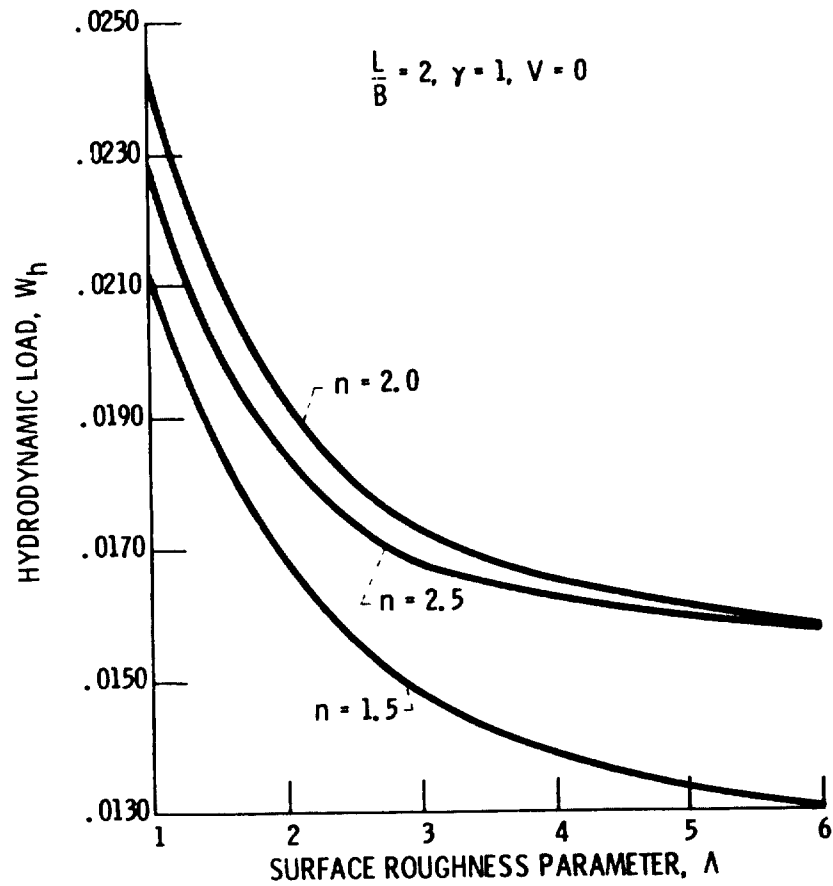


Figure 6. - Variation of hydrodynamic load with surface roughness parameter for various attitudes.

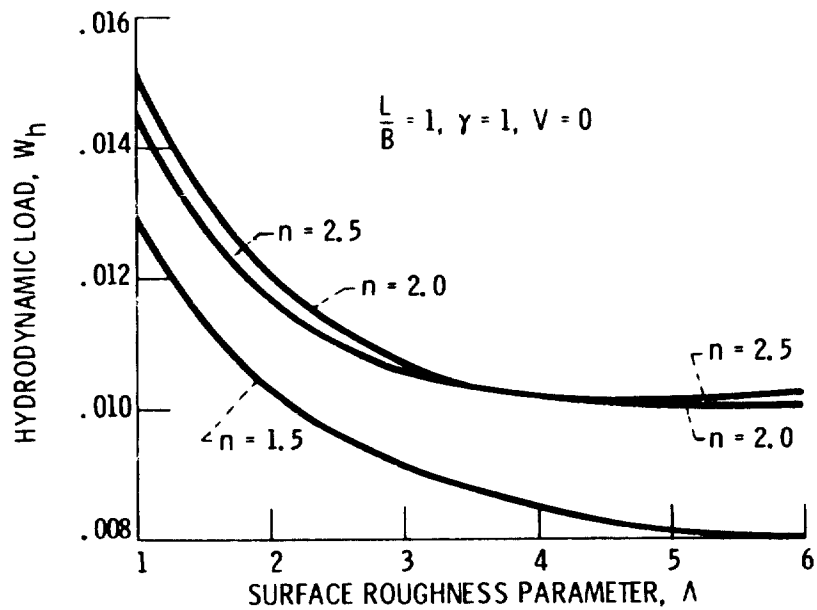


Figure 7. - Variation of hydrodynamic load with surface roughness parameter for various attitudes.

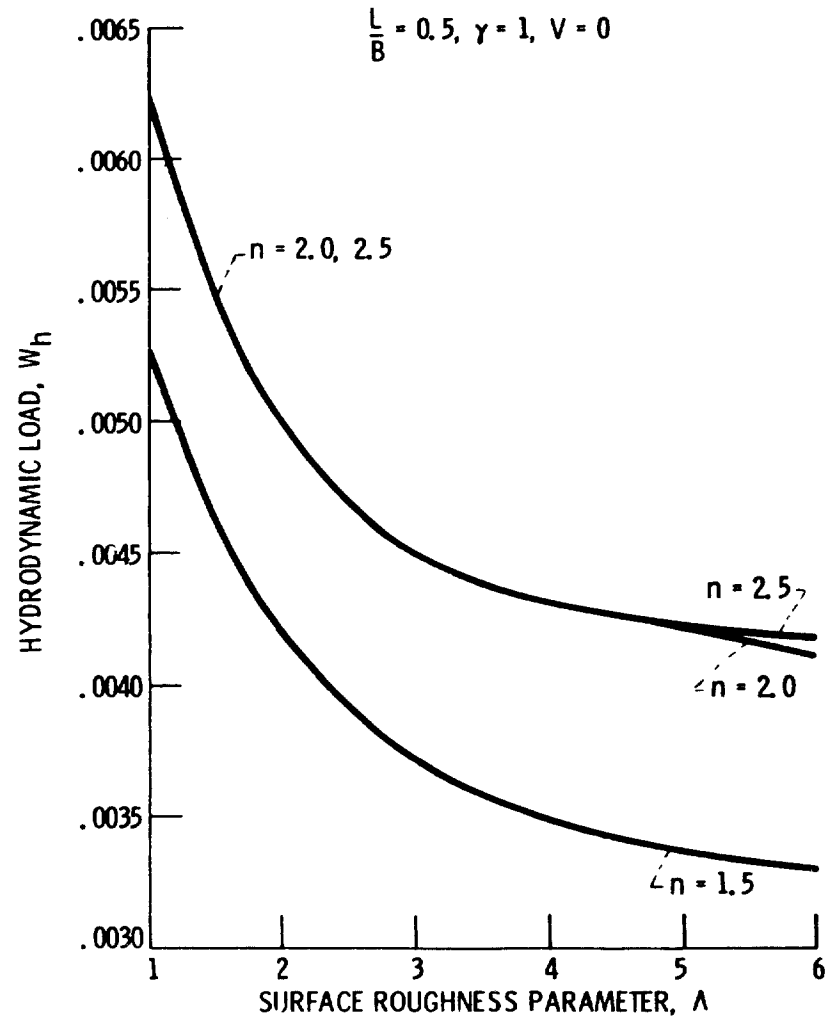


Figure 8. - Variation of hydrodynamic load with surface roughness parameter for various attitudes.

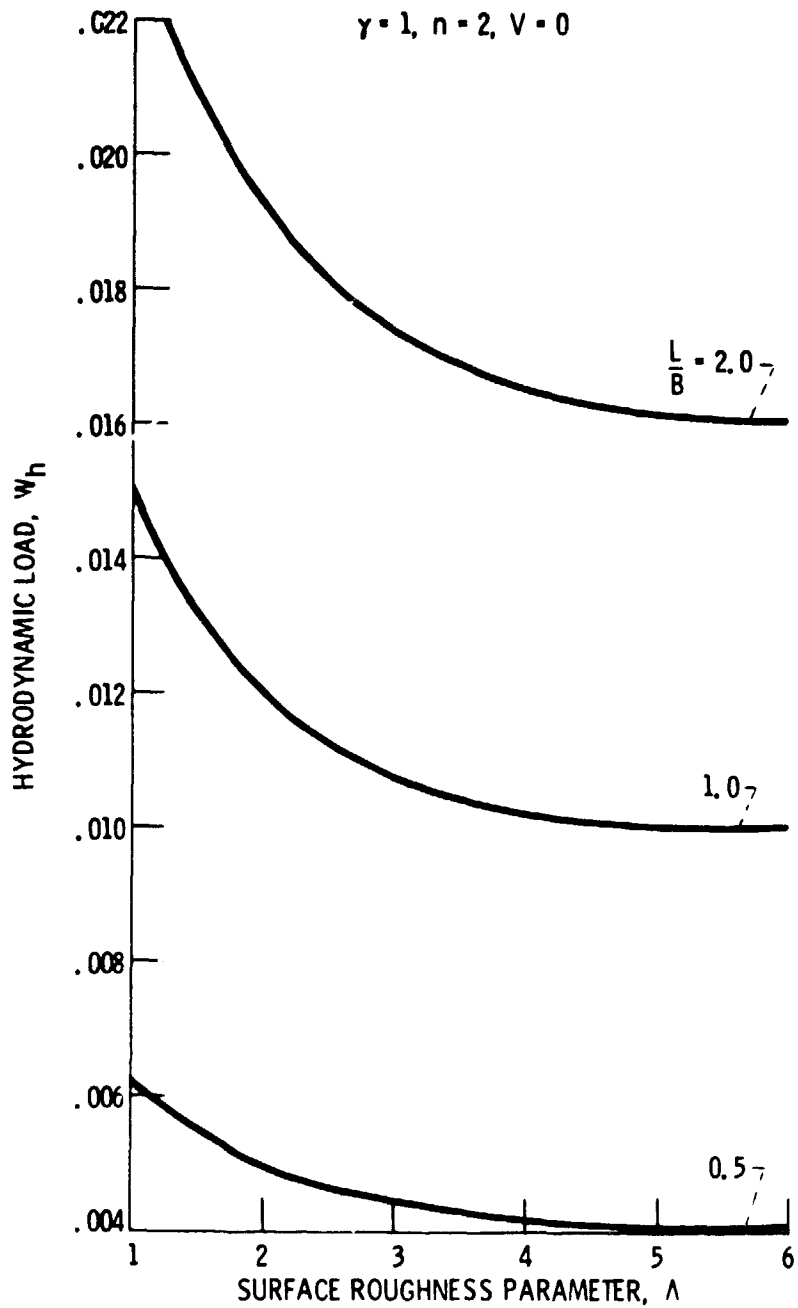


Figure 9. - Variation of hydrodynamic load with surface roughness parameter for various  $L/B$  ratios.

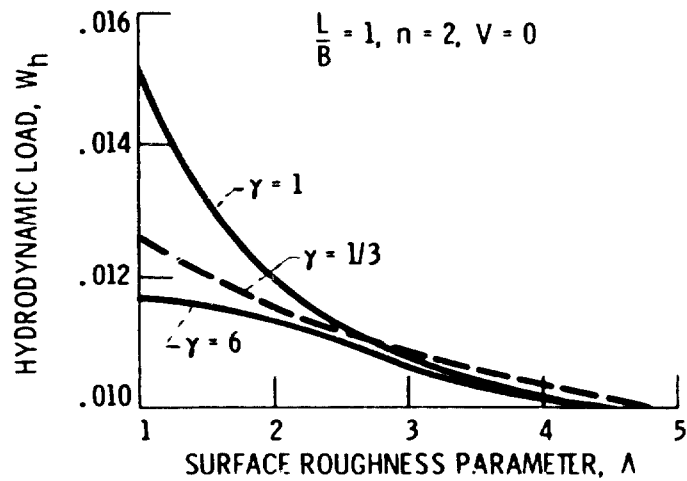


Figure 10. - Variation of hydrodynamic load with roughness parameter for various surface patterns.

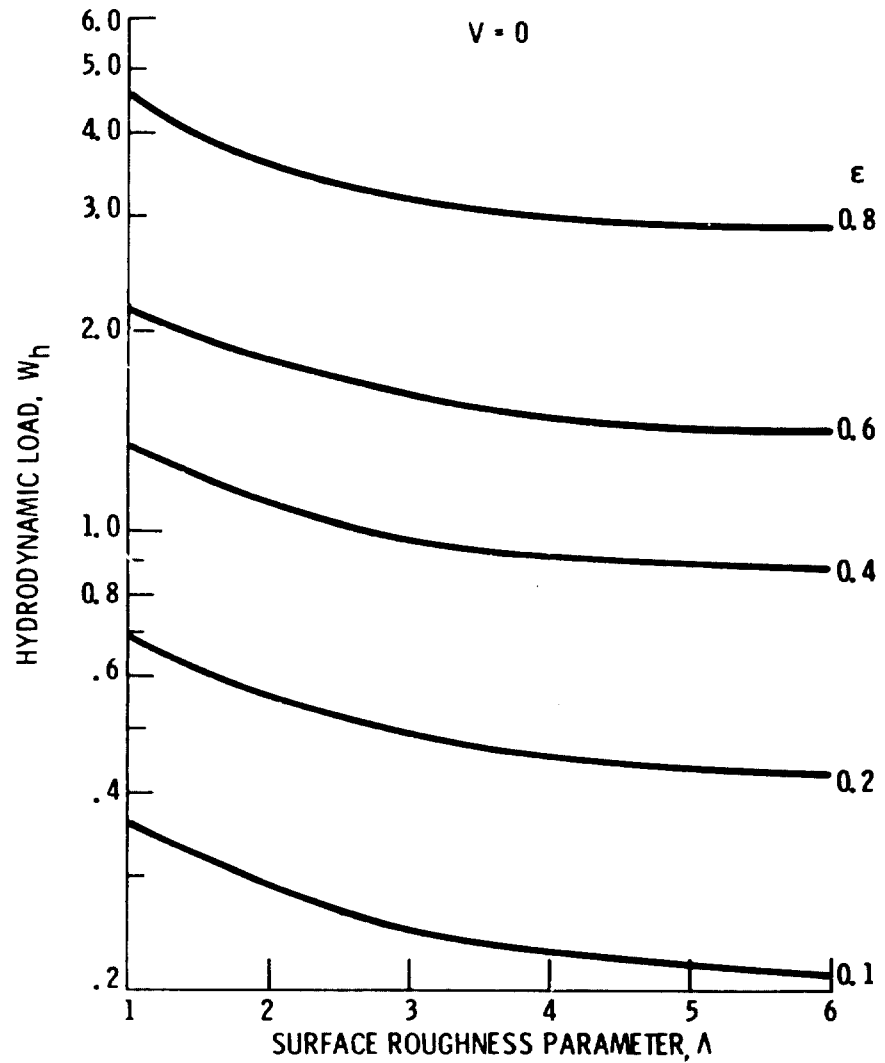


Figure 11. - Variation of load of an infinitely long journal bearing with roughness parameter for various eccentricity ratios ( $V = 0$ ).



1 Report No. <b>NASA TM-81711</b>	2 Government Accession No.	3 Recipient's Catalog No.
4 Title and Subtitle <b>EFFECT OF SURFACE ROUGHNESS ON HYDRODYNAMIC BEARINGS</b>	5 Report Date	6 Performing Organization Code <b>505-32-42</b>
	7 Author(s) <b>Bankim C. Majumdar and Bernard J. Hamrock</b>	8 Performing Organization Report No. <b>E-698</b>
9 Performing Organization Name and Address <b>National Aeronautics and Space Administration Lewis Research Center Cleveland, Ohio 44135</b>	10 Work Unit No.	11 Contract or Grant No.
	12 Sponsoring Agency Name and Address <b>National Aeronautics and Space Administration Washington, D. C. 20546</b>	13 Type of Report and Period Covered <b>Technical Memorandum</b>
14 Sponsoring Agency Code		
15 Supplementary Notes <b>Prepared for the Joint Lubrication Conference cosponsored by the American Society of Mechanical Engineers and the American Society of Lubrication Engineers, New Orleans, Louisiana, October 5-7, 1981.</b>		
16 Abstract <p>A theoretical analysis on the performance of hydrodynamic oil bearings is made considering surface roughness effect. The hydrodynamic as well as asperity contact load is found. Assuming the surface height distribution as Gaussian the contact pressure is calculated. The average Reynolds equation of partially lubricated surface is used to calculate hydrodynamic load. An analytical expression for average gap is found and is introduced to modify the average Reynolds equation. The resulting boundary value problem is then solved numerically by finite difference methods using the method of successive over-relaxation. The pressure distribution and hydrodynamic load capacity of plane slider and journal bearings are calculated for various design data. The effects of attitude and roughness of surface on the bearing performance are shown. The results are compared with similar available solution of rough surface bearings. It is shown that (1) the contribution of contact load is not significant and (2) the hydrodynamic and contact load increase with surface roughness.</p>		
17 Key Words (Suggested by Author(s)) <b>Surface roughness Hydrodynamic lubrication Slider bearing Journal bearing</b>	18 Distribution Statement <b>Unclassified - unlimited STAR Category 37</b>	
19 Security Classif. of this report <b>Unclassified</b>	20 Security Classif. of this page <b>Unclassified</b>	21 No. of Pages
		22 Price*